

Normal Vibrations of Potassium Iodide

G. DOLLING, R. A. COWLEY, C. SCHITTENHELM,* AND I. M. THORSON

Chalk River Nuclear Laboratories, Atomic Energy of Canada Limited, Chalk River, Ontario, Canada

(Received 17 February 1966)

The frequency/wave vector dispersion relation $\nu_j(\mathbf{q})$ for the normal modes of vibration of pure potassium iodide at 90°K has been measured by inelastic neutron scattering techniques. The experiments were performed with both a time-of-flight machine and a triple-axis crystal spectrometer. The results obtained from the latter spectrometer have been analyzed in terms of various interionic-force models. A satisfactory fit to the results is provided by an eleven-parameter dipole approximation model, which allows for the polarizability of both ions. Comparison of normal-mode frequencies calculated from this model with those observed in the time-of-flight experiments shows generally good agreement. The frequency distribution function for the normal modes, computed from the best-fit model, displays a well-defined energy gap, from 8.65 to 11.85 meV, separating the acoustic and optic modes. The moments of this function are in excellent agreement with values derived from heat-capacity data. By assuming an exponential form for the nearest-neighbor short-range force constants, the temperature variation of the thermal expansion, and the frequency shift and inverse lifetime of the transverse optic mode of very long wavelength, have been calculated and compared with the available experimental results. The occurrence of localized impurity modes in the energy gap in the frequency distribution for potassium iodide doped with potassium nitrite is briefly discussed.

I. INTRODUCTION

THE frequency/wave vector relation $\nu_j(\mathbf{q})$ (j is a polarization index) of several alkali halides has been studied both experimentally and theoretically in recent years.¹ The most complete experimental investigations to date have been made of sodium iodide² and potassium bromide,³ by techniques of coherent inelastic neutron scattering from single-crystal specimens. In these experiments, a collimated monoenergetic beam of slow neutrons (energy E_0 , wave vector \mathbf{k}_0) is incident on the specimen. Coherent scattering processes in which one phonon of the lattice vibrations is either created or annihilated are governed by two conservation conditions⁴:

$$\mathbf{k}_0 - \mathbf{k}' = \mathbf{Q} = 2\pi\boldsymbol{\tau} + \mathbf{q}, \quad (1)$$

$$E_0 - E' = \pm h\nu, \quad (2)$$

where primed quantities refer to the scattered neutrons and $\boldsymbol{\tau}$ is a vector of the reciprocal lattice of the crystal. Thus the energy distribution of the scattered neutrons consists (in this approximation) of a small number of delta-function peaks at which Eqs. (1) and (2) may be satisfied simultaneously with the dispersion relation $\nu = \nu_j(\mathbf{q})$ for the normal modes of vibration. In practice these peaks are broadened partly by instrumental resolution and partly by anharmonic effects^{5,6} which limit the lifetime of the normal modes.

The particular interest of potassium iodide arises from the large ionic mass ratio I^-/K^+ ($= 3.25$) which leads

one to expect a clear separation in energy between the acoustic and optic modes of vibration; the possibility then arises of localized impurity modes whose energy falls within this gap for suitable impurities. Observations of such "gap modes" have recently been made by optical⁷ and infrared⁸⁻¹¹ absorption techniques.

Although the abovementioned experiments on NaI and KBr were both performed with a triple-axis spectrometer,¹² other types of instrument may also be used,¹³ for example, a phased-rotor, time-of-flight spectrometer. Experiments carried out on the triple-axis machine at facility C5 of the NRU reactor, Chalk River, and on the phased-rotor spectrometer¹⁴ at facility E2 of the same reactor, are described in Sec. II.

In Sec. III the results are analyzed in terms of various dipole approximation models^{3,15} for the interionic forces in KI. A good fit to almost all the results, and also to the measured refractive index¹⁶ and elastic constants,¹⁷ may be obtained with a model which takes into account the polarizability of both ions, axially symmetric short-range forces between first and second nearest-neighbor ions, and a variable ionic charge. In Sec. IV, this model is used to calculate the frequency distribution

⁷ T. Timusk and W. Staude, *Phys. Rev. Letters* **13**, 373 (1964).

⁸ A. J. Sievers and C. D. Lytle, *Phys. Letters* **14**, 271 (1965).

⁹ K. F. Renk, *Phys. Letters* **14**, 281 (1965).

¹⁰ A. J. Sievers, A. A. Maradudin, and S. S. Jaswal, *Phys. Rev.* **138**, A272 (1965).

¹¹ H. Bilz, K. F. Renk, and K. H. Timmesfeld, *Solid State Commun.* **3**, 223 (1965).

¹² B. N. Brockhouse, in *Proceedings of the Symposium on Inelastic Scattering of Neutrons in Solids and Liquids, Vienna, 1960* (International Atomic Energy Agency, Vienna, 1961), p. 113.

¹³ Reference 1, Chaps. II and III.

¹⁴ P. A. Egelstaff, S. J. Cocking, and T. K. Alexander, in *Proceedings of the Symposium on Inelastic Scattering of Neutrons in Solids and Liquids* (International Atomic Energy Agency, Vienna, 1963), p. 165.

¹⁵ R. A. Cowley, W. Cochran, B. N. Brockhouse, and A. D. B. Woods, *Phys. Rev.* **131**, 1030 (1963).

¹⁶ K. Højendahl, *Kgl. Danske Videnskab. Selskab, Mat. Fys. Medd.* **16**, No. 2 (1938).

¹⁷ W. W. Scales, *Phys. Rev.* **112**, 49 (1958).

* N.R.C. Postdoctoral Fellow.

¹ This subject is reviewed in *Thermal Neutron Scattering*, edited by P. A. Egelstaff (Academic Press Inc., New York, 1965), Chap. V.

² A. D. B. Woods, W. Cochran, and B. N. Brockhouse, *Phys. Rev.* **119**, 980 (1960).

³ A. D. B. Woods, B. N. Brockhouse, R. A. Cowley, and W. Cochran, *Phys. Rev.* **131**, 1025 (1963).

⁴ G. Placzek and L. Van Hove, *Phys. Rev.* **93**, 1207 (1954).

⁵ A. A. Maradudin and A. E. Fein, *Phys. Rev.* **128**, 2589 (1962).

⁶ R. A. Cowley, *Advan. Phys.* **12**, 421 (1963).

function $g(\nu)$ for the normal modes of vibration in KI, together with its moments. As expected, this $g(\nu)$ displays a well-defined energy gap, separating the optic and acoustic modes. An extension to the model to take into account anharmonic effects in a simple manner⁶ permits the calculation of the temperature dependence of the thermal expansion and of the frequency shift and inverse lifetime of the transverse optic mode of very long wavelength. A brief discussion is also given of the spectrum of localized modes which has been observed⁷⁻⁹ in specimens of KI containing KNO_2 impurity.

II. EXPERIMENTS

Two series of experiments were performed to measure the phonon dispersion relation $\nu_j(\mathbf{q})$ for a single crystal¹⁸ of pure KI maintained at a temperature of 95°K in an evacuated cryostat. The crystal was in the shape of a cylinder, 5 cm×2 cm diameter, and had a mosaic spread of 0.4°. As mentioned in Sec. I, two different instruments were employed, a triple-axis crystal spectrometer and a phased-rotor spectrometer, both at the NRU reactor, Chalk River. In both series of experiments, the (110) crystallographic plane of the specimen was in the plane of the incident and scattered neutron beams. The use of the "constant-Q" mode of operation¹² in the former experiments allowed measurements to be made of phonons with wave vectors lying along directions of high symmetry, whereas the phased-rotor experiments in general gave results in off-symmetry directions within the (110) plane.

1. Triple-Axis Crystal-Spectrometer Experiments

A description of this spectrometer and its modes of operation has been given previously¹² and will not be repeated here. Measurements were made of the frequencies of normal modes of vibration propagating along the three directions of highest symmetry, Δ , Σ and Λ (i.e., $[00\zeta]$, $[\zeta\zeta 0]$, and $[\zeta\zeta\zeta]$, respectively, where ζ is a reduced wave-vector coordinate such that $\zeta=1$ at the zone boundary point X). The complete results are shown in Fig. 1, and some typical frequencies are listed in Table I. Almost all the measurements were made under conditions of neutron energy loss, with the scattered neutron energy fixed at 0.0164 eV, and the method of "constant-Q" was utilized throughout. This enables the frequency of a mode of any preselected wave vector to be measured in a convenient and direct manner. One advantage of this lies in the comparative ease with which results for special wave vectors, e.g., those along the high symmetry directions, may be analyzed theoretically.

Owing to the relatively large mosaic spread of the specimen, it was frequently possible to observe peaks in the scattered neutron distributions which would be

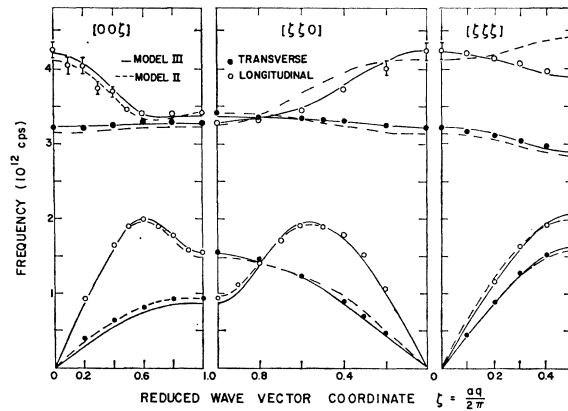


FIG. 1. Dispersion relation for normal modes of vibration propagating along three directions of high symmetry in KI at 95°K. Open (filled) circles denote longitudinal (transverse) modes. Experimental errors are given by the diameters of the circles if no error bars are shown. The dashed curves are the best fit to the results on the basis of a simple three-parameter dipole approximation model, model II, while the continuous curves refer to an 11-parameter model, model III.

associated with a very low or zero cross section if only single scattering processes were involved (for example, one-phonon scattering involving modes of vibration with polarization vectors normal to the plane containing the incident and scattered neutron beams). Such spurious peaks usually result from double-scattering processes,¹⁹ either elastic "Bragg" followed by inelastic one-phonon scattering or vice versa. This difficulty was also experienced in the phased-rotor spectrometer experiments discussed below. Nevertheless, we believe that the results given here are substantially correct.

2. Phased-Rotor Spectrometer Experiments

The principle of operation of the phased-rotor spectrometer has been described previously¹⁴ but some details of the apparatus used in these experiments will be given to allow a comparison with the triple-axis crystal spectrometer. Normally, two curved-slot metal rotors placed 0.80 and 3.54 m from the NRU reactor face define the bursts of neutrons incident on a specimen

TABLE I. Frequencies of selected normal modes in KI at 95°K.

Wave-vector coordinates	Branch	Frequency (10 ¹² cps)
(0, 0, 0)	LO	4.26±0.10
	TO	3.21±0.04
(1.0, 0, 0)	LO	3.38±0.05
	TO	3.28±0.05
	LA	1.56±0.03
	TA	0.94±0.03
(0.5, 0.5, 0.5)	LO	3.94±0.06
	TO	2.93±0.03
	LA	2.06±0.05
	TA	1.65±0.04

¹⁸ The crystal was purchased from the Harshaw Chemical Company through the good offices of Professor T. Timusk.

¹⁹ Reference 1, p. 206.

0.50 m beyond the second rotor. Two resin-fiberglass secondary rotors remove fast neutrons from the beam at 0.19 and 1.87 m from the reactor, but do not affect the pulse shape. To improve the incident beam intensity for these measurements the primary rotors were placed at 1.87 and 3.54 m from the reactor and rotors with slot curvature 1.41 rad/m rotating at 390 cps (about vertical axes) were used. The 12 slot rotors (2.5-mm slot width) delivered a beam of 2.5×10^4 neutrons/sec over an area 2.5 cm high by 5.1 cm wide at the specimen position. One standard deviation on the time of arrival of the neutrons at the specimen was 4.0 μ sec and on their reciprocal velocities 2.0 μ sec/m. To detect the scattered neutrons twelve 5-cm diameter Li⁶F (ZnS) scintillators on 2-in. diam EMI 6097B photomultipliers were positioned in the horizontal plane 2.98 m from the specimen. Groups of three detectors were placed at scattering angles around 69°, 85°, 101°, and 117° to the incident beam direction.

Pulse-shape discriminator circuits²⁰ and paraffin and cadmium shielding reduced the background rate in the detectors to ≈ 2 counts/min. The background depended smoothly on rotor-phase. The events from each detector were sorted into 270 4- μ sec time channels initiated by a pulse from a phototube at a particular phase point in each cycle of the last rotor. The reciprocal velocity or wavelength scale was determined by sorting events from fission chambers placed directly in the beam before and after the specimen.

The data were recorded on a magnetic tape for subsequent sorting and readout on to punched cards. The processing of the data was then done on a Control Data Corporation G-20 computer. The peaks in the time-of-flight distribution were found and the phonon frequency ν and reduced wave vector \mathbf{q} corresponding to these peaks calculated, together with the probable errors on these quantities arising from the experimental geometry factors and peak statistics.

Data were taken for 100 to 150 h for each of 12 different combinations of incident neutron energy (0.055 to 0.070 eV) and specimen orientation Ψ (Ψ is the angle between the incident beam and the [001] crystallographic axis of the specimen). The experiments defined approximately 160 neutron groups corresponding to normal modes in the frequency range $1.0 \rightarrow 4.2 \times 10^{12}$ cps. Several spurious peaks were also observed which probably arose from the double scattering processes mentioned in Sec. III. A very large number of low-frequency peaks were also observed, with relatively poor precision ($> 5\%$); difficulty was experienced in many of these cases in resolving the various peaks from each other and from neutrons scattered elastically from aluminum radiation shields surrounding the specimen.

Since the vast majority of phonons were in off-symmetry directions, they could not readily be utilized

in the force model analyses described in Sec. III. However, they form a valuable check on the reliability of force models based only on data for the high-symmetry directions. A comparison of some observed and calculated phonon frequencies for general wave vectors is given in Sec. IV.

III. THE MODELS

The frequencies of the normal modes propagating in symmetry directions, as determined by the triple-axis spectrometer experiments described in Sec. III, have been used to obtain the parameters of several different models for the dynamics of potassium iodide. Most of these models were dipole-approximation or shell models, similar to those which were successful in describing the normal mode frequencies of sodium iodide and potassium bromide.^{2,15} A detailed description of these models is not presented here since several accounts are now available. The detailed definitions of the parameters used below are given by Cochran *et al.*²¹

The parameters of both the dipole-approximation models and the simpler rigid-ion models were obtained by least-squares fitting to the experimental measurements in the three symmetry directions, and to the measured elastic constants¹⁷ and the high-frequency dielectric constant.¹⁶ The results for many of the models were, not surprisingly, similar in form to those already described for sodium iodide and potassium bromide. The parameters of three models are shown in Table II.

Model I is a seven-parameter rigid-ion model and the agreement obtained with experiment is surprisingly good. Presumably the ionic charge of 0.63 should be considered as a kind of "effective" charge for the lattice dynamics which in some sense takes account of the polarizability of the ions. Model II is a simple three-parameter dipole approximation model which is compared with the experimental results in Fig. 1. As found earlier^{2,15} this model gives considerable discrepancies for the Σ and Λ longitudinal optic modes. Model III is an eleven-parameter model which gives good agreement with the measurements for most of the branches of the dispersion relation, as shown in Fig. 1, and with the elastic and dielectric constants as given in Table III. The parameters of this model show very similar features to the best models obtained for potassium bromide and sodium iodide: the positive-ion short-range polarizability is negative, while the electrical polarizabilities are shared more equally between the ions than expected from the tables of Tessman *et al.*²² These features undoubtedly arise from the neglect of the quadrupole distortions of the ions as discussed for potassium bromide.¹⁵ Models were also fitted in which the short-range \mathbf{T} matrix was allowed to differ from the \mathbf{R} matrix, in a similar way to that employed

²¹ W. Cochran, R. A. Cowley, G. Dolling, and M. M. Elcombe, Proc. Roy. Soc. (London) (to be published).

²² J. R. Tessman, A. H. Khan, and W. Shockley, Phys. Rev. **92**, 890 (1953).

²⁰ L. A. Wraight, Harwell Report AERE-M833, 1965 (unpublished).

TABLE II. Parameters of three different models of the interionic forces in KI.

Model	A ($e^2/2v$)	B ($e^2/2v$)	A^1 ($e^2/2v$)	B^1 ($e^2/2v$)	A^{11} ($e^2/2v$)	B^{11} ($e^2/2v$)
I	10.1 ± 0.1	-0.48 ± 0.06	0.18 ± 0.06	0.02 ± 0.05	0.16 ± 0.035	0.16 ± 0.03
II	13.78 ± 0.404	-1.165	0	0	0	0
III	13.4 ± 0.5	-1.0 ± 0.2	-0.16 ± 0.25	-0.01 ± 0.06	-0.29 ± 0.24	0.05 ± 0.05
	Z (e)	α_1 (10^{-24} cm ³)	d_1 (e)	α_2 (10^{-24} cm ³)	d_2 (e)	X mean fitting error
I	0.63 ± 0.01	0	0	0	0	3.56
II	1.0	0	0	7.50 ± 0.1	0.322 ± 0.007	5.74
III	0.92 ± 0.04	2.28 ± 0.145	-0.11 ± 0.04	4.51 ± 0.4	0.13 ± 0.05	1.65

for lead telluride.²¹ No significant improvement in the agreement with experiment was obtained.

IV. CALCULATIONS WITH MODELS

The best-fit parameters of model III obtained in the previous section have been used to calculate several properties of potassium iodide, and these calculations compared with the available experimental measurements. Firstly the frequencies of the off-symmetry modes determined on the phased-rotor spectrometer, described in Sec. II2, were calculated from this model. The over-all agreement between the calculations and the experiment was good, and a comparison of some of the best experimental results with the calculations is shown in Table IV. The discrepancies between the model and the experiment were not found to be significantly greater than normal in any particular regions of reciprocal space. We can therefore have confidence that the model does give a good description of the frequencies of the normal modes over the whole of the (110) plane, and it seems likely that the same is true for normal modes throughout the Brillouin zone. The frequency distribution has therefore been calculated using the extrapolation method²³ to obtain 48 009 024 frequencies in the full Brillouin zone. The result is shown in Fig. 2. The calculation confirms that there is a gap in the frequency distribution, between 2.09 and 2.87 (in units of 10^{12} cps). This frequency distribution has been used to calculate the temperature dependence of the specific

heat and Debye temperature. The latter is compared with the experimental measurements of Berg and Morrison²⁴ in Fig. 3. Figure 4 shows a comparison of the moments of the frequency distribution, expressed in the form of "equivalent Debye frequencies," as compared with those deduced from the specific-heat measurements.^{24,25} In spite of the neglect of anharmonic effects in these calculations, the agreement with experiment is very good.

The frequency distribution function of KI has been calculated by Karo and Hardy²⁶ on the basis of a modified version of the dipole approximation model fitted only to the compressibility, the static dielectric constant and the Raman frequency. (The relationship of this model to other dipole approximation models is discussed in detail in Ref. 15.) Since this model does not

TABLE III. Comparison of observed and calculated properties of KI.

Property	Model III calculation	Experiment	Reference
Elastic constant, (10^{11} dyn/cm)	C_{11} 3.28 C_{12} 0.33 C_{44} 0.382	3.21 ± 0.03 0.31 ± 0.04 0.369 ± 0.004	17 17 17
High-frequency dielectric constant	ϵ_∞ 2.41	2.71 ± 0.10 ^a	16 ^a

^a The room-temperature value quoted is 2.69; the value 2.71 is estimated assuming the same temperature dependence as that of KBr.

²³ G. Gilat and G. Dolling, Phys. Letters 8, 304 (1964).

TABLE IV. A selection of normal-mode frequencies ν_{obs} (units 10^{12} cps) measured with the phased-rotor spectrometer, compared with calculations from model III. The reduced wave-vector coordinates ζ_x ($=\zeta_y$) and ζ_z are given in units of $(2\pi/a)$ where a is the lattice constant. Negative values of ν_{obs} denote neutron energy-gain processes.

ζ_x	ζ_z	ν_{obs}	ν_{calc}
0.35	0.24	4.06 ± 0.10	3.973
0.36	0.12	3.92 ± 0.08	3.910
0.36	0.01	3.83 ± 0.11	3.869
0.31	0.81	3.50 ± 0.08	3.548
0.37	0.15	3.23 ± 0.08	3.178
0.10	0.43	3.14 ± 0.10	3.164
0.46	0.10	-2.00 ± 0.10	1.900
0.40	0.53	1.93 ± 0.11	2.007
0.45	0.33	1.92 ± 0.08	1.969
0.39	0.76	1.89 ± 0.11	1.922
0.16	0.61	-1.79 ± 0.08	1.925
0.40	0.18	1.77 ± 0.08	1.795
0.26	0.34	1.64 ± 0.10	1.584
0.35	0.52	1.63 ± 0.09	1.589
0.25	0.68	-1.59 ± 0.09	1.495
0.24	0.82	1.51 ± 0.09	1.526
0.54	0.10	-1.24 ± 0.09	1.212

²⁴ W. T. Berg and J. A. Morrison, Proc. Roy. Soc. (London) A242, 467 (1957).

²⁵ T. H. K. Barron and J. A. Morrison, Proc. Roy. Soc. (London) A256, 427 (1960).

²⁶ A. M. Karo and J. R. Hardy, Phys. Rev. 129, 2024 (1963).

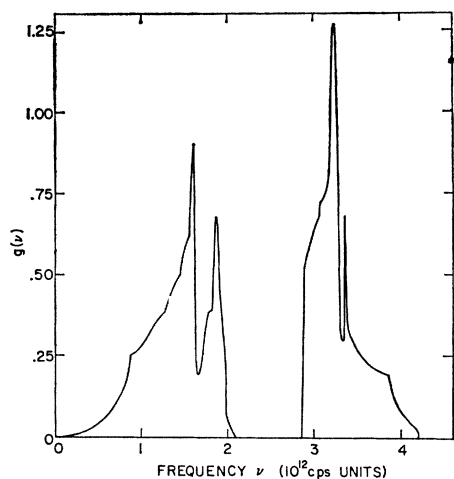


FIG. 2. Frequency distribution function, $g(\nu)$, for the normal modes of vibration of KI, computed from the best-fit model III. The energy gap separating the optic and acoustic branches is clearly defined.

provide a satisfactory fit to the measured dispersion curves, the derived distribution function is less accurate than that shown in Fig. 2. The location of the energy gap, for example, is about 10% lower than given by the present calculations.

Considerable success has been obtained^{6,27} in calculations of the anharmonic properties of sodium iodide and potassium bromide, with aid of a simple extension to models that are similar to those obtained above. The anharmonicity is assumed to arise from the nearest-neighbor short-range interaction, which furthermore may be described by a potential, $\phi = \beta \exp(-r/\rho)$. The parameters ρ and β can be obtained from the

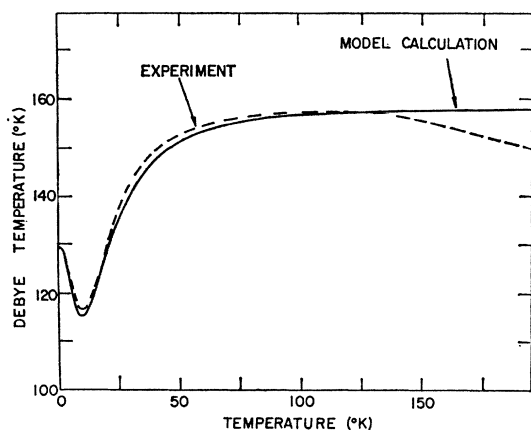


FIG. 3. The Debye temperature of KI as a function of temperature, computed from the harmonic model III, (continuous curve) and compared with values derived from heat-capacity data²⁴ (dashed curve).

²⁷ E. R. Cowley and R. A. Cowley, Proc. Roy. Soc. (London) **A287**, 259 (1965).

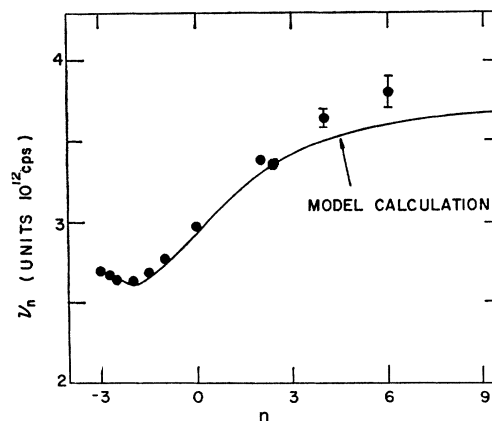


FIG. 4. Equivalent "Debye" frequencies computed from the moments of the distribution function (Fig. 2) and compared with values (filled circles) derived from heat-capacity data.²⁴

nearest-neighbor short-range parameters A and B , and hence the calculations made without the introduction of further parameters. We have performed similar calculations for potassium iodide for the thermal expansion, and for the frequency shifts and inverse lifetimes (or widths) of the optic modes of nearly zero wave vector. The results are summarized in Table V, where they are compared with the available experimental results. The agreement with experiment is comparable with that obtained for sodium iodide, namely that the effects of anharmonicity are overestimated by about 10–20%, but this is not too surprising in view of the approximations involved. It is probably worth commenting that the longitudinal optic mode is influenced to a much greater degree by anharmonicity than the transverse mode, as is the case also for sodium iodide and potassium bromide.

TABLE V. Observed values for some properties of KI, compared with calculations based on an anharmonic-force model.

Property	Temperature (°K)	Calculations	Experiment	Ref.
Thermal expansion ($10^{-6}/^{\circ}\text{K}$)	30	0.91	1.08	a
	90	3.42		a
	200	4.04	3.78	a
	300	4.13	4.20	a
Frequency of TO mode at $q=0$ (10^{12} cps)	5	3.27	3.25	b
	90	3.21	3.21	This paper ^c
	200	3.07		
	300	2.98	2.95	d
	300		3.04	b
Inverse lifetime of TO mode (10^{12} cps)	5	0.011	0.090	b
	90	0.043		
	200	0.083		
	300	0.124	0.104	b

^a B. Yates and C. H. Panter, Proc. Phys. Soc. (London) **80**, 373 (1962).

^b G. O. Jones, D. H. Martin, P. A. Mawer, and C. H. Perry, Proc. Roy. Soc. (London) **A261**, 10 (1961).

^c The calculations are fitted to this value.

^d R. B. Barnes, Z. Physik **75**, 723 (1932).

V. DISCUSSION

1. Experimental Methods

The study of crystal dynamics by means of coherent one-phonon scattering of neutrons from single crystals requires (i) the observation of distinct peaks in the energy distributions of scattered neutrons, (ii) the identification of the mode j of the phonon associated with each peak, and (iii) the analysis of the measured phonon frequencies in terms of various theoretical models. These requirements may be most easily met by studying wherever possible a selection of normal modes which propagate along directions of high symmetry in the crystal. The scattering cross section associated with creation or annihilation of a phonon is a function of its frequency and polarization vector. Hence we may identify an observed peak by comparing its intensity with the calculated cross section. This calculation may be made much more easily, frequently merely by inspection, if the symmetry of the mode is sufficiently high. Similarly, the analysis of results described in Sec. III is much simpler for high-symmetry modes. Naturally, a device that enables the direct and convenient study of pre-selected modes, such as a triple-axis crystal spectrometer, enjoys substantial advantages over devices which do not. The observation of distinct peaks, rather than several unresolved peaks, is also facilitated by careful selection of the modes to be studied. For these reasons, the results obtained with the triple-axis spectrometer were analyzed more fully than those from the phased-rotor spectrometer.

The chief advantage of the phased-rotor type of spectrometer lies in the possibility it affords of accumulating large amounts of data covering a wide (if random) selection of phonons. However, a large fraction of observed peaks corresponds to low-frequency phonons which have a high scattering cross section. High-frequency modes tend to be under represented. A fully automatic data-handling system is necessary to sift the

information and select the most useful results. In this paper, these results have been used only as a check on the reliability of theoretical models fitted to symmetry-direction data. Even for this purpose, the assignment of the peaks to particular branches could not always be made unambiguously. Although the least-squares fitting procedure could be extended in principle to include non-symmetry direction modes, in practice the increase in computing time involved would be almost prohibitive at present. Further discussion of advantages and disadvantages of the two types of spectrometer for various kinds of experiment may be found in Ref. 1, pp. 71, 137, and 196.

2. Local Modes in Potassium Iodide

Recently, several observations have been made⁷⁻⁹ of localized modes of vibration in KI containing small amounts of KNO_2 . A calculation of the vibration frequency of the NO_2^- ion in the KI lattice, on the basis of simple mass-defect theories,¹⁰ indicated that it would probably fall in the gap in the frequency distribution function of the host. In practice, a complex spectrum of localized modes is observed, which is believed^{8,11} to be associated with various rotational degrees of freedom of the NO_2^- ion. The present experiments and calculations give the location of the energy gap in pure KI with a precision of 2 or 3%, and confirm that the local modes of the KI: KNO_2 system do in fact fall within that gap.

ACKNOWLEDGMENTS

We would like to thank Dr. A. D. B. Woods for helpful advice and assistance and Professor T. Timusk and Professor A. A. Maradudin for their encouragement. We are indebted to D. H. C. Harris, E. A. Glaser, B. Booty, M. McManus, W. J. McKay, and F. Tomaiuolo for their expert technical assistance.